eppendorf

Boost Your (Stem) Cell Culture

We assist you to scale up your bioprocess –
Eppendorf Bioprocess Solutions for Cell & Gene Therapy Development - Flexibe, Scalable, Industrial

The BioFlo® 320 offers flexibility, better control, and maximum functionality while occupying a fraction of the valuable lab space of similar systems. This means greater efficiency and productivity at a lower operating cost for your lab. BioBLU® Single-Use Bioreactors were developed as true replacements for existing reusable vessels.

- > Sterility Assurance Level (SAL): 10^{-6}
- > Simplified handling reduces cross-contamination
- > Reliable scalability from 250 mL - 40 L through industrial design
- > Proven for animal and human cell lines
- > Increased productivity with reduced turnaround time between runs

www.eppendorf.com/BioBLUc

Eppendorf®, the Eppendorf Brand Design, and BioBLU® are registered trademarks of Eppendorf SE, Germany. BioFlo® is a registered trademark of Eppendorf, Inc., USA. All rights reserved, including graphics and images.
Copyright ©2023 by Eppendorf SE.

Check for updates

Received: 1 December 2022 | Revised: 31 March 2023 | Accepted: 1 April 2023

DOI: 10.1002/bit.28402

ARTICLE

BIOTECHNOLOGY AND BIOENGINEERING WILEY

Process economics evaluation and optimization of adeno-associated virus downstream processing

Annabel Lyle[1] | Christos Stamatis[1] | Thomas Linke[2] | Martyn Hulley[3] | Albert Schmelzer[2] | Richard Turner[3] | Suzanne S. Farid[1]

[1]Department of Biochemical Engineering, The Advanced Centre for Biochemical Engineering, University College London, London, UK

[2]Biopharmaceuticals Development, R&D, AstraZeneca, Gaithersburg, Maryland, USA

[3]Biopharmaceuticals Development, R&D, AstraZeneca, Cambridge, UK

Correspondence

Suzanne S. Farid, Department of Biochemical Engineering, University College London, Gower St, London WC1E 6BT, UK.
Email: s.farid@ucl.ac.uk

Funding information

AstraZeneca; Engineering and Physical Sciences Research Council; University College London

Abstract

Adeno-associated virus (AAV) manufacturing has traditionally focused upon lab-scale techniques to culture and purify vector products, leading to limitations in production capacity. The tool presented in this paper assesses the feasibility of using non-scalable technologies at high AAV demands and identifies optimal flowsheets at large-scale that meet both cost and purity targets. The decisional tool comprises (a) a detailed process economics model with the relevant mass balance, sizing, and costing equations for AAV upstream and downstream technologies, (b) a built-in Monte Carlo simulation to assess uncertainties, and (c) a brute-force optimization algorithm for rapid investigation into the optimal purification combinations. The results overall highlighted that switching to more scalable upstream and downstream processing alternatives is economically advantageous. The base case analysis showed the cost and robustness advantages of utilizing suspension cell culture over adherent, as well as a fully chromatographic purification platform over batch ultracentrifugation. Expanding the set of purification options available gave insights into the optimal combination to satisfy both cost and purity targets. As the purity target increased, the optimal polishing solution moved from the non-capsid purifying multimodal chromatography to anion-exchange chromatography or continuous ultracentrifugation.

KEYWORDS

adeno-associated vectors, chromatography, cost of goods modeling, Monte Carlo simulation, optimization, ultracentrifugation

1 | INTRODUCTION

It has been widely proven that adeno-associated viruses (AAVs) are a competent delivery system of genetic material into cells. Currently, from a recorded set of 1140 clinical trials utilizing viral vectors as an in vivo gene therapy, 250 of these used AAVs (Bulcha et al., 2021). AAVs have also achieved commercial success, with the approval of Luxturna (Spark Therapeutics), Zolgensma (AveXis), and more recently Roctavian (BioMarin), Hemgenix (CSL Behring), and Upstaza (PTC Therapeutics). However, these products are often associated with antiquated methods for manufacturing, which incur high production costs. This paper presents the development of a tool to map out and evaluate various AAV flowsheets and compare the resulting cost of goods (COG) per dose and purity performance.

This is an open access article under the terms of the Creative Commons Attribution License, which permits use, distribution and reproduction in any medium, provided the original work is properly cited.
© 2023 The Authors. *Biotechnology and Bioengineering* published by Wiley Periodicals LLC.

Traditionally, recombinant AAVs have been successfully produced to high titers in a laboratory setting, particularly using adherent human embryonic kidney (HEK293) cells (Xiao et al., 1998). At similar scales, purification via gradient density ultracentrifugation (UC) has enabled consistently high yields and purities (Dobrowsky et al., 2021). As a result, such labaratory procedures are often directly translated for use in a commercial setting, despite these technologies being characteristically laborious and costly to maintain at the large scale (Dobrowsky et al., 2021; van der Loo & Wright, 2016). For example, batch ultracentrifugation cannot be scaled in the same manner as chromatography, thus manufacturers must often resort to scaling out, by increasing the number of ultracentrifuges employed. Despite this difficulty, the step is still reportedly employed in clinical and commercial manufacture (Glover et al., 2019; Wright, 2008). Therefore, there exists the need for the effective translation of the purification performance achieved with technologies such as ultracentrifugation at the lab scale, to more scalable technologies that are economically feasible in a commercial setting.

A significant and somewhat unique impurity issue that arises with AAV manufacturing is the generation of vector particles lacking fully packaged genetic material, referred to as empty or partially-filled capsids. As a result, this type of viral particle cannot provide the same clinical benefit as a full capsid and it is thought that, in some cases, administration may provoke an increased immune response (Wright, 2014a) or reduce the expression of the desired gene (Hebben, 2018). Empty capsids present an additional product-related impurity that is necessary to remove for ensuring batch-to-batch product consistency (Wang et al., 2019). The challenge industry faces is that empty capsids are structurally closely related to the full capsids (Qu et al., 2015), thereby making it difficult to utilize some chromatographic procedures and exploit molecular and structural differences between impurities. This similarity is exemplified by the inability of affinity chromatography to remove empty capsids, as the ligand cannot distinguish between full and empty capsids due to identical capsid properties (Nass et al., 2018). It has been shown that ion-exchange chromatography (IEX) can adequately address this impurity issue for some serotypes (Nass et al., 2018; Qu et al., 2015), as there is a subtle difference in the isoelectric point between full and empty capsids (approximately 0.4 units) (Qu et al., 2015). Having said this, IEX has exhibited a wide range in yields, as evidenced by the data in Supporting Information: Table S1. Furthermore, steps such as ultracentrifugation have demonstrated success in removal of empty particles, independent of AAV serotype (Crosson et al., 2018) and allow for more stable yields relative to IEX. This fact therefore presents the trade-off between ultracentrifugation and IEX; that is a high yield and purity step against a scalable strategy respectively. Alternative scalable options include the use of continuous ultracentrifugation, which can allow for large product volumes to be processed (Chen et al., 2016). In terms of purity, final product specifications lack definition with respect to empty capsids and hence there remains ambiguity around target removal levels. In contrast, information exists on AAV process-related impurities such as host cell proteins (HCP) and host cell DNA, where Wright (2014b) provided data on target levels for both.

The application of decisional tools has proved vital for capturing key process-business trade-offs, and rapid mapping of cost-effective bioprocesses from often large decision spaces. Whilst there have been studies capturing process economic modeling of viral vectors, there is a smaller pool of economics studies focusing on AAVs. Masri et al. (2019) carried out an assessment of the suitability of current manufacturing technologies for AAV and lentivirus production. Furthermore, Comisel et al. (2021b) presented a decisional tool for the evaluation of the most cost-effective lentiviral vector processes, particularly with a comparative focus on the upstream processing (USP) portion of the bioprocess. This tool highlighted the importance of moving to more scalable upstream options from a cost perspective, as suspension was shown to achieve a significant COG reduction over more traditional technologies. This work was later extended to include a comparison between transient transfection and stable producer cell lines to generate viral vector products (Comisel et al., 2021a). Specifically pertaining to AAVs, an upstream cost evaluation was conducted, comparing multiple cell culture technologies, including both adherent and suspension platforms, to identify which technology gave the minimum COG per dose (Cameau et al., 2020). To date, there has not been an in-depth analysis of whole flowsheets with both upstream and downstream manufacturing strategies for AAV from both economic and purity perspectives.

This paper investigates the cost-effectiveness of AAV manufacturing strategies, evaluating both USP and downstream processing (DSP). Section 4.1 provides the deterministic analysis, focusing upon adherent cell factories (CF10) versus suspension stirred tank bioreactors for cell culture, and batch ultracentrifugation against anion-exchange chromatography (AEX) for polishing purification comparison. Section 4.2 outlines how the dose size affects this base case COG/dose ranking. Furthermore, an uncertainty analysis was carried out to compare the robustness of the different manufacturing strategies in Section 4.3. Finally, an optimization of AAV purification platform was implemented in Sections 4.4 and 4.5 to find the optimal capture and polishing options from an economic and purity perspective.

2 | MATERIALS AND METHODS

2.1 | Description of decisional tool

The decisional tool in Figure 1 was developed to allow for a comparison of AAV process flowsheets and ultimately determination of cost-effectiveness, whilst meeting any imposed purity constraints and targets. The tool comprised a process economics model, with an uncertainty analysis feature for assessment under stochastic conditions. Additionally, a brute-force optimization algorithm fed information into the process economics model, where outputs were then fed back for identification of the optimal output. The tool was implemented in Python 3.7 (Python Software Foundation) and used Microsoft Excel (Microsoft Corporation) for an adjoining database which contained many of the inputs that are outlined in Figure 1, namely much of the mass balance, sizing cost, and market data.

10970290, 0, Downloaded from https://onlinelibrary.wiley.com/doi/10.1002/bit.28402 by University College London UCL Library Services, Wiley Online Library on [26/04/2023]. See the Terms and Conditions (https://onlinelibrary.wiley.com/terms-and-conditions) on Wiley Online Library for rules of use; OA articles are governed by the applicable Creative Commons License

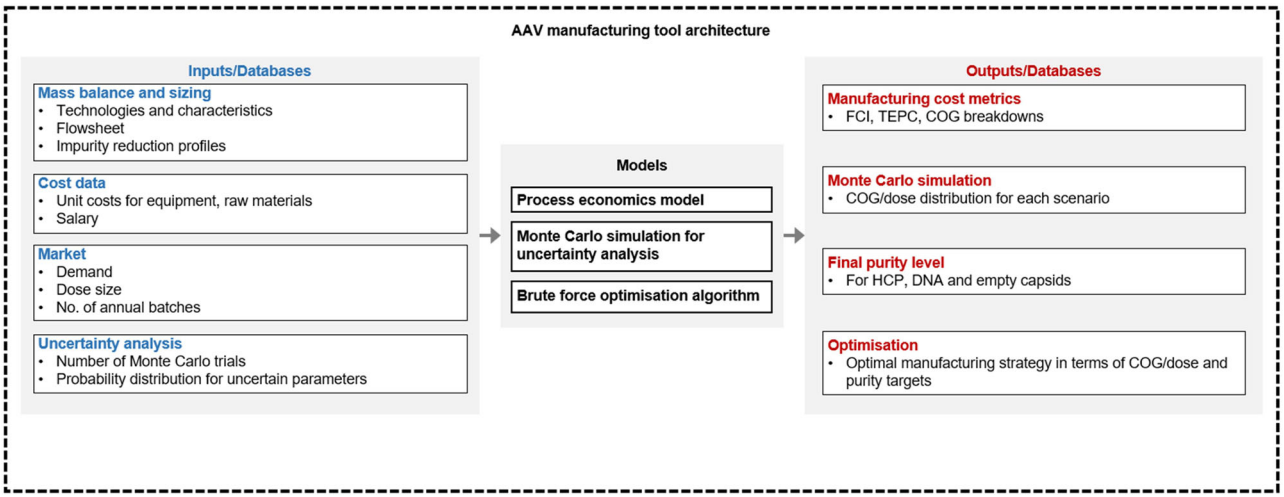

FIGURE 1 Decisional tool architecture used for the AAV process economics case study. FCI, fixed capital investment; COG, cost of goods; TEPC, total equipment purchase cost.

2.1.1 | Process economics model

The process economics model utilized throughout the case study is comprised of process models for various unit operations derived from Simaria et al. (2012) and Stamatis and Farid (2021). Key viral vector process models, particularly fill-finish, were adapted from Comisel et al. (2021a), but altered to represent AAV manufacturing over lentiviral vectors. In terms of fixed capital investment (FCI), the method described by Pereira Chilima et al. (2020) was utilized to determine the facility footprint and hence the overall FCI.

The model allowed for a whole flowsheet mass balance, as well as equipment sizing for each unit operation and ancillary equipment. The cost assumptions stored in the aforementioned database were used in parallel with process models to calculate costs including raw materials (reagents, consumables, QCQA), labor and facility-related indirect costs for any given process flowsheet. These constituent costs were used to find the total COG for both the drug substance (DS) and drug product (DP) stages. A breakdown of these costs can be found in Supporting Information: Table S1. Furthermore, the annual demand (number (no) of doses) was utilized with the total COG to ascertain the COG per dose.

$$\text{COG/dose} = \frac{c_{\text{mat,annual}} + c_{\text{lab,annual}} + c_{\text{ind,annual}}}{N_{\text{dose,annual}}} \quad (1)$$

where $c_{mat,annual}$ is the total annual cost of materials (both for the process and QC), $c_{lab,annual}$ is the total annual labor cost, $c_{ind,annual}$ is the total annual indirect cost, and $N_{dose,annual}$ is the annual number of doses.

2.1.2 | Stochastic analysis

The uncertainty analysis via Monte Carlo simulation was applied to pivotal process parameters deemed to be the most variable in a realistic AAV bioprocess. Utilization of the Monte Carlo method required each uncertain input parameter to have a probability distribution assigned to it. A random value from each uncertainty distribution was drawn and replaced the deterministic input value. Convergence testing of the standard deviation was used to determine the number of trials (500) required to capture the impact of uncertainty on the outputs.

2.1.3 | Brute-force optimization

The brute-force optimization algorithm was used to simulate a plethora of AAV flowsheet combinations and ultimately identify what the optimal flowsheet was in terms of minimum COG and satisfying varying purity targets. The algorithm evaluated each flowsheet within the process economics model one at a time and generated the corresponding COG/dose, whilst consistently screening for and hence updating the minimum value until all in the set had been assessed. In terms of purity, the algorithm allowed for multiple starting or target impurity levels to be defined, serving as additional criteria for brute-force solutions to satisfy. Integer values were assigned to both the unit operations and the possible technologies that could be selected at each stage to aid in formulating the set for the algorithm to work upon.

3 | CASE STUDY SETUP

3.1 | Case study overview

The tool outlined in Section 2 was used to evaluate the economic and operational performance of various AAV flowsheets, initially from a small set of alternatives, before expanding the decision space to include a myriad of other processing options. The study began with exploring the impact of scalability during cell culture and at polishing purification, using a fixed demand of 1000 doses per year and a dose size of 1×10^{14} vg/dose. The range of dose sizes seen in marketed

10970290, 0, Downloaded from https://onlinelibrary.wiley.com/doi/10.1002/bit.28402 by University College London UCL Library Services, Wiley Online Library on [26/04/2023]. See the Terms and Conditions (https://onlinelibrary.wiley.com/terms-and-conditions) on Wiley Online Library for rules of use; OA articles are governed by the applicable Creative Commons License

products and in late phase clinical trials across a range of indications were studied and the median of this range was used in the base case analysis. The base case demand was derived as the average of expected commercial patient populations (Masri et al., 2019). For cell culture, the trade-off between adherent and suspension culture was evaluated with adherent culture offering higher AAV productivities (vg/cell) and suspension culture offering better scalability. For polishing purification, batch UC was compared to AEX chromatography to assess the trade-off between UC delivering higher yield and purity (with respect to empty capsid removal) but being less scalable relative to AEX. The solution set was later expanded to include more purification platform options for evaluation in terms of cost and meeting increasing purity targets.

The process economics model was used to generate the deterministic COG/dose across demands for the different scenarios, before a Monte Carlo simulation was used to capture the robustness of the scenarios. The optimization algorithm was later used to identify the most cost-effective flowsheet that met target purities.

3.2 | Process outline

The various process flowsheets initially evaluated in this case study are shown in Figure 2, which includes a dendrogram to illustrate the key differences explored in the cell culture and polishing stages. The preliminary case study investigated two alternatives for USP, adherent or suspension cell culture. For the adherent scenario, multi-layer cell factories (e.g., Cell Factory™) were used, specifically the 10-layer model (CF10), with a surface area totaling 6360 cm^2 per unit. Moreover, the production culture vessel of choice in the suspension case was a stirred-tank single-use bioreactor (SUB), whereby the size was selected from the calculated working volume required.

The USP duration assumed was 5 days, whereby cells were seeded at the beginning of Day 1 at a density of 25,000 cells/cm^2 for adherent and 125,000 cells/mL for suspension. Post-cell culture, harvest by TFF occurred, where the product stream was the cells as is the case with intracellular AAVs. Intracellular AAV flowsheets also contain a chemical lysis step, whereby cells are lysed by addition of detergent to rupture the plasma membranes, resulting in release of the product along with the generation of cell debris. This debris is removed by a clarifying depth filter stage post-lysis.

Regarding purification, AFF featured as the capture stage in the first case study, supplemented by a traditional iodixanol gradient density UC polishing stage in some cases, or an AEX chromatography in others. For UC, one batch ultracentrifuge unit (e.g., Type 70Ti rotor; Beckman Coulter) was assumed to have a maximum rotor capacity of 312 mL and was allowed to be operated for a maximum of two cycles per working day. As discussed in Section 1, UC has been shown to be successful at removing empty capsids generated in AAV processing, a product-related impurity known to be characteristically difficult to eliminate via other means. Due to slight pI differences between full and empty capsids, AEX has also been shown to give an adequate empty capsid removal—thus it was chosen as the scalable comparator against UC. Moreover, as also evidenced in Supporting Information: Table S1, AEX yield can be variable and is often lower than what can be achieved by UC, thereby introducing the polishing

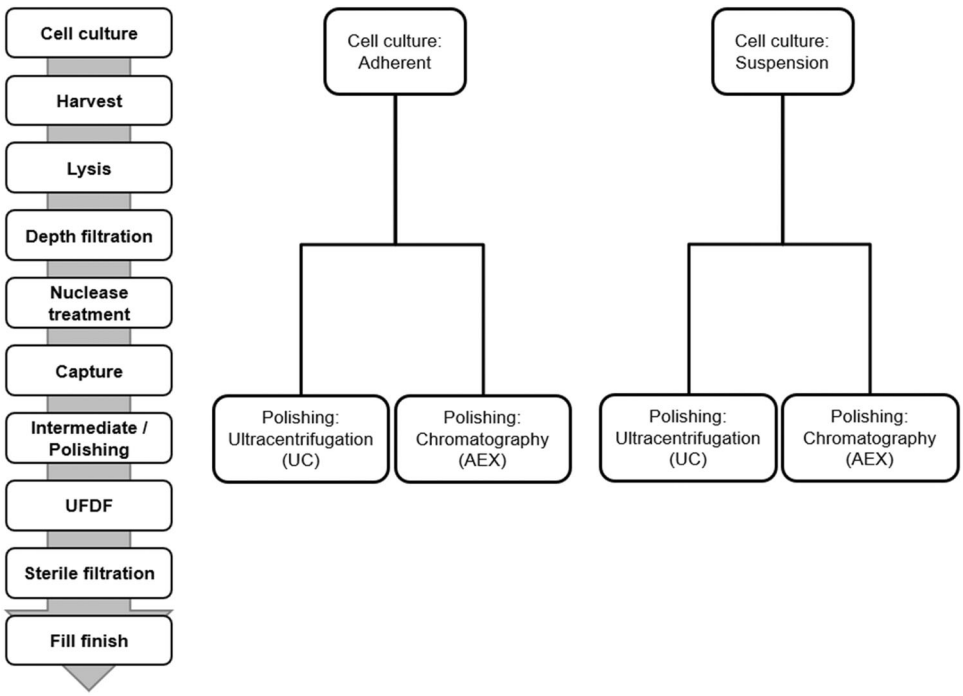

FIGURE 2 Viral vector process flowsheet for adeno-associated virus (AAV) vector product. The dendrograms illustrate the key differences between the four flowsheets initially evaluated in the cell culture (adherent v suspension) and polishing (ultracentrifugation v chromatography) stages. AEX, anion-exchange chromatography; UC, ultracentrifugation.

10970290, 0, Downloaded from https://onlinelibrary.wiley.com/doi/10.1002/bit.28402 by University College London UCL Library Services, Wiley Online Library on [26/04/2023]. See the Terms and Conditions (https://onlinelibrary.wiley.com/terms-and-conditions) on Wiley Online Library for rules of use; OA articles are governed by the applicable Creative Commons License

purification trade-off of UC with higher purity and yield versus scalable chromatography.

3.3 | Key assumptions

Table 1 shows the scenario specific assumptions used. Due to the dependency on cell culture type to describe titers, the titers were expressed in vg/cm^2 and vg/L for adherent and suspension, respectively. The cell productivity was used to calculate the titer and was chosen as the basis for comparison between scenarios. Furthermore, due to the differences in polishing purification between UC and AEX scenarios, the process yield differed between flowsheets, with UC assumed to result in a higher value. The key assumptions for the various unit operations employed across all scenarios can be found in Tables 2 and 3. Additionally, the active facility days was assumed to be 330. It was also assumed a maximum of 30 batches could be carried out per year per train, where one train was defined as one SUB through to fill-finish, with allowances for multiple units of certain DSP unit operations to run in parallel (e.g., UC).

Additionally, Table 2 outlines the extra material required for QCQA purposes at both DS and DP, which was assumed to be a percentage in both cases. These values were sourced from Masri et al. (2019). Conversely, a fixed volume method for estimating QCQA demands has also been utilized in the literature, notably in Comisel et al. (2021b). The model outputs from using either method differ depending on the dose size under consideration, where the fixed volume method results in a significant portion of product fluid being retained at smaller dose sizes. The impact of using either method is further discussed in Section 4.2.

3.4 | Monte Carlo assumptions

The uncertain input parameters used in the Monte Carlo simulation, along with their corresponding probability distributions are displayed alongside the results. These include titers and the polishing purification yields, due to their characteristic variability in AAV manufacturing. The ranges set for each variable were selected from a

TABLE 2 Key AAV process assumptions for the case-study.

Category	Parameter	Value
General	Dose size (vg/dose)	1×10^{14}
	Maximum batches per train	30
	Facility active days	330
	DSP shifts	3
Seed & production cell culture	Seeding cell density (adherent) (cells/cm^2)	2.5×10^4
	Seeding cell density (suspension) (cells/mL)	1.25×10^5
	Medium cost ($/L)	100
	Cell culture duration (days)	5
	Doubling time (days)	1
	Plasmid DNA requirement (μg/10^6 cells)	1
	Transfection mix cost (pDNA + PEI) ($/g)	190,000
Chemical lysis	Step yield	98%
	Lysis buffer requirement (L/L)	100
Depth filtration	Step yield	95%
	Filter capacity (L/m^2)	60
	Flux (LMH)	100
Nuclease treatment	Benzonase requirement (U/mL)	50
	Benzonase activity (U/μL)	250
	Benzonase cost ($/25,000 U)	230
UFDF/TFF	Step yield	95%
	Flux (LMH)	60
	Duration (concentration and diafiltration) (h)	6
Sterile filtration	Step yield	90%
	Flux (LMH)	40
Drug substance/ drug product	DP concentration (vg/mL)	1×10^{13}
	Extra material produced for DS	10%
	Extra material produced for DP	10%

Abbreviation: DSP, downstream processing.

TABLE 1 AAV flowsheet combinations considered in the deterministic analysis and the associated assumptions for each.

Flowsheet abbreviation	Cell culture technology	Polishing stage	Cell productivity (vg/cell)	Titer	Harvest cell density	Overall process yield (%)
Ad-UC	Adherent	Ultracentrifugation	120,000	2.4×10^{10} vg/cm^2	2×10^5 cells/cm^2	29
Ad-AEX	Adherent	AEX	120,000	2.4×10^{10} vg/cm^2	2×10^5 cells/cm^2	25
Susp-UC	Suspension	Ultracentrifugation	60,000	6×10^{13} vg/L	1×10^6 cells/mL	29
Susp-AEX	Suspension	AEX	60,000	6×10^{13} vg/L	1×10^6 cells/mL	25

Abbreviations: AEX, anion-exchange chromatography; UC, ultracentrifugation.

10970290, 0, Downloaded from https://onlinelibrary.wiley.com/doi/10.1002/bit.28402 by University College London UCL Library Services, Wiley Online Library on [26/04/2023]. See the Terms and Conditions (https://onlinelibrary.wiley.com/terms-and-conditions) on Wiley Online Library for rules of use; OA articles are governed by the applicable Creative Commons License

review of the relevant literature, as well as industrial correspondence (see Supporting Information: Table S1).

3.5 | Optimization assumptions

A series of options were identified and selected as part of determining the optimal AAV flowsheet from a cost and purity perspective (Table 3). Only capture and polishing purification unit operations were assessed (however, in three step purification cases, intermediate purification was also studied). Special conditions were assumed for a three-step purification process; a third step was only added where the two-step platform did not possess empty capsid removal capabilities, and, hence, a third step that did allow for such removal was added to bolster purification performance. Namely, this was only identified to occur for an affinity and multimodal combination and would only be followed by AEX.

For the purity aspect of the optimization framework, empty capsids represent a product-related impurity unique to the AAV space and in a relatively nascent field, final targets are not well defined. In contrast, specifications for HCP and DNA are more clearly defined in literature, as these impurities have been well documented and tracked in other modality areas (derived from cell culture). For the case study, both HCP and DNA were assessed at two starting levels, termed low (L) and high (H). The target levels for HCP and DNA were assumed to be 100 ng/mg and 10 ng per dose, respectively (Bracewell et al., 2015; Wright, 2020). The low starting levels for HCP and DNA were assumed to be 2×10^{-7} and 6×10^{-10} ng/vg. For the high starting levels, the values were assumed to be 2×10^{-5} ng/vg for HCP and 6×10^{-8} ng/vg for DNA. For empty capsids, a single starting level was evaluated, however three potential targets were assessed, terms low (L), medium (M), and high (H).

This optimization case study first evaluated the optimal strategy when one AEX yield was considered. The evaluation was then extended by illustrating how the optimal solution changes if varying AEX yields are encountered, as well as empty capsid reduction requirement. For this study, a suspension cell culture was assumed for each flowsheet option. In addition, the demand and number of annual batches were fixed throughout.

4 | RESULTS AND DISCUSSION

The decisional tool introduced in Section 2 was utilized to evaluate the economic advantages that can be obtained from adapting to more scalable manufacturing strategies. This was initially addressed deterministically, before an uncertainty analysis was introduced to account for process variability and to assess the robustness of the base case. Finally, the last part of the case study identifies the optimal manufacturing strategy in terms of both cost and purity targets from a broader set of alternatives.

4.1 | What is the COG/dose breakdown for traditional versus scalable AAV flowsheets?

The impact of the key traditional versus scalable USP and DSP choices for AAV flowsheets on the COG/dose was explored initially. Figure 3 presents the COG/dose comparison between the initial four flowsheets studied at a demand of 1×10^{17} vg/year. These four flowsheets were adherent-UC (Ad-UC), adherent-AEX (Ad-AEX), suspension-UC (Susp-UC), and suspension-AEX. Overall, suspension-AEX (Susp-AEX) was shown to be the most cost-effective out of the set, offering a ~40% reduction over the most expensive flowsheet, which was Ad-UC. This cost was driven by lower labor and equipment requirements associated with the use of one suspension bioreactor and one AEX column and skid versus multiple units in the competing flowsheets. The materials cost was not found to be a significant driver across scenarios. Furthermore, relative to the traditional flowsheet of Ad-UC, the competing manufacturing strategies were found to allow for a 17%–41% reduction in COG/dose.

Figure 3 also provides insights on the COG drivers for each flowsheet. Comparing solely UC and AEX scenarios, DSP labor costs were higher for Ad-UC than Ad-AEX due to the condition that one operator can handle a maximum of two ultracentrifuges per run. Twenty-three ultracentrifuges were required in parallel for Ad-UC, thus an additional 12 DSP operators were necessary for this flowsheet. This requirement evidently also resulted in a greater DSP indirect cost than Ad-AEX, as a larger total equipment purchase cost and facility footprint were associated with numerous ultracentrifuges compared to a single AEX column and skid. This trend was similarly observed when comparing Susp-UC and Susp-AEX. Similarly, studying adherent versus suspension cell culture scenarios, cost differences were largely driven by labor costs. The Ad-UC and Ad-AEX required the use of 78–91 cell factory (CF10) units with 16–18 USP operators, in comparison to the 2 operators used in the suspension flowsheets with a 250 L bioreactor (Susp-UC or Susp-AEX).

The trends observed can, to some extent, be described by examining the USP:DSP cost ratios. In general, it was shown that DSP costs dominated the COG, with the exception to this being Ad-AEX, where USP:DSP was found to be 54%:46%. The impact of UC on the DSP costs was highlighted by the distinct shift in cost ratios from Ad-UC to Ad-AEX or Susp-UC to Susp-AEX. From a DSP perspective, this shift was from 64%–77% to 46%–65%. In terms of USP ratios, moving from an adherent to a suspension platform lowers the USP cost contribution from 36%–54% to 23%–35%, thus highlighting the significance of moving to more scalable platforms upon the COG.

In summary, a suspension flowsheet coupled with AEX provided the most cost-effective strategy relative to other options explored, reinforcing the importance of moving to scalable strategies when in a commercial manufacturing environment. Having said this, the results here represent a single instance of demand and dose size, thus it became desirable to evaluate the cost-effectiveness of the flowsheets across dose size and demands.

10970290, 0, Downloaded from https://onlinelibrary.wiley.com/doi/10.1002/bit.28402 by University College London UCL Library Services, Wiley Online Library on [26/04/2023]. See the Terms and Conditions (https://onlinelibrary.wiley.com/terms-and-conditions) on Wiley Online Library for rules of use; OA articles are governed by the applicable Creative Commons License

TABLE 3 Purification assumptions utilized in the process economics model.

Technology	Abbreviation	Commercial equivalent	Step yield	DBC (vg/mL[a])	Resin cost ($/L)	HCP reduction (LRV)	DNA reduction (LRV)	EC reduction (%)	Ultracentrifuge cost ($)	Step
Affinity chromatography (high DBC)	AFFH	Poros AAVX (Thermo Fisher Scientific)	70%	3×10^{13}	50,000	4	2.5	N/A	N/A	Capture
Affinity chromatography (low DBC)	AFFL	AVB Sepharose (Cytiva)	70%	3×10^{12}	25,000	4	2.5	N/A	N/A	Capture
Anion exchange chromatography	AEX	Poros 50HQ (Thermo Fisher Scientific)	60%	5×10^{13}	2500	2.5	1.5	70%	N/A	Capture, polishing
Cation exchange chromatography	CEX	Poros 50HS (Thermo Fisher Scientific)	55%	5×10^{13}	2500	2.5	1.5	N/A	N/A	Capture, polishing
Multimodal chromatography	MM	Capto Core 400 (Cytiva)	75%	13 (mg/mL)	4500	2	0.5	N/A	N/A	Capture, intermediate, polishing
Batch ultracentrifugation	BatchUC	Type 70Ti (Beckman Coulter)	70%	N/A	N/A	3	3	95%	85,000	Capture, polishing
Continuous ultracentrifugation	ContiUC	KII Model (Alfa Wassermann)	70%	N/A	N/A	3	3	95%	350,000	Capture, polishing

Abbreviations: AEX, anion-exchange chromatography; CEX, cation exchange chromatography; DBC, dynamic binding capacity; HCP, host cell proteins; MM, multimodal chromatography; UC, ultracentrifugation.

[a]Unless otherwise stated.

10970290, 0, Downloaded from https://onlinelibrary.wiley.com/doi/10.1002/bit.28402 by University College London UCL Library Services, Wiley Online Library on [26/04/2023]. See the Terms and Conditions (https://onlinelibrary.wiley.com/terms-and-conditions) on Wiley Online Library for rules of use; OA articles are governed by the applicable Creative Commons License

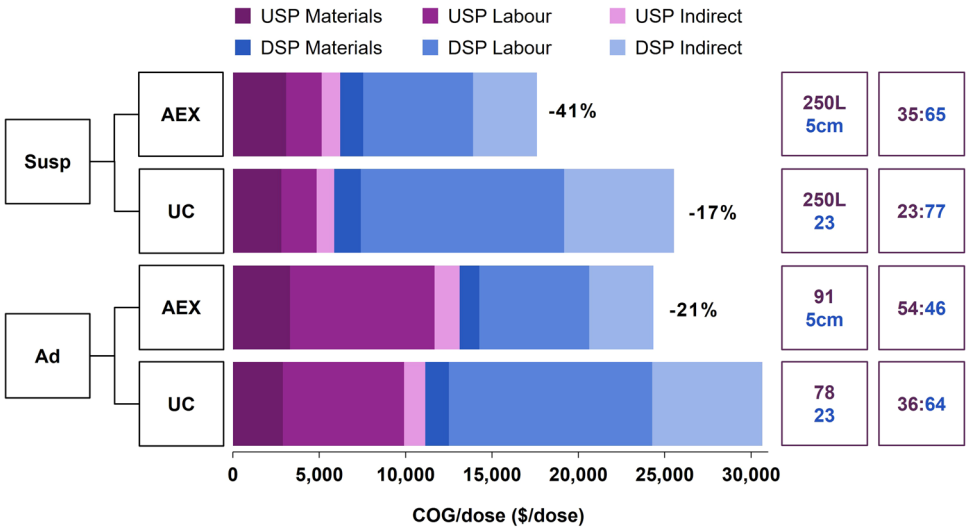

FIGURE 3 COG/dose breakdown by category within USP and DSP process stages for four AAV flowsheet options with adherent or suspension culture for USP and AEX or UC for polishing. The boxes on the right of each bar represent key sizing metrics; the top number highlights the number of cell culture units or the bioreactor volume (for adherent or suspension scenarios, respectively). The bottom number represents the number of parallel ultracentrifuges used or the AEX column diameter (for UC or AEX scenarios, respectively). The second set of boxes located to the right of the bars highlights the USP:DSP cost of goods ratios for each scenario. The percentages next to each bar represent the COG/dose reduction for each flowsheet relative to the traditional flowsheet of adherent-UC. The demand was assumed to be 1000 doses/year, with a dose size of 1×10^{14} vg/dose. The facility was resized for each set of inputs. Ad, adherent culture; AAV, adeno-associated virus; AEX, anion-exchange chromatography; COG, cost of goods; DSP, downstream processing; Susp, suspension culture; UC, ultracentrifugation; USP, upstream processing.

4.2 | How does dose size impact COG/dose?

The required dose of AAV varies significantly based on therapeutic indication, with ophthalmic indications at the lower end (e.g., 1×10^{12} vg/dose) through to neuromuscular and hemophilia indications at the higher end (e.g., 1×10^{15} vg/dose). Hence, scalability is a more significant issue for those companies targeting diseases with characteristically high dose sizes. Figure 4 displays the impact of dose size from 1×10^{12} to 1×10^{15} vg/dose upon flowsheet ranking. The optimal technology changes from AEX options in either adherent (Ad-AEX) or suspension (Susp-AEX) mode at the low doses to Susp-AEX being the clear winner at the higher doses.

Little difference was found between Ad-AEX and Susp-AEX at dose sizes of 1×10^{13} vg/dose or lower, as Ad-AEX required 10 CF units per batch or less, needing only two USP operators as with the Susp-AEX scenario. This result suggests that for indications corresponding to these dose sizes, most notably ophthalmic genetic diseases, conducting adherent cell culture presents no extra financial burden to a company relative to suspension. Conversely, an increasing dose size accentuates the COG differences between suspension and adherent cultures. At 1×10^{15} vg/dose, the ranking alters such that Ad-AEX becomes less economically viable than either suspension scenarios, due to the increase in CF units and hence labor requirement. This suggests that for indications requiring a large dose size (e.g., neuromuscular and hemophilia), adherent is a less attractive cell culture option.

Further to the discussion of QCQA material in Section 3.1, the impact of using either a fixed volume or percentage approach is dose size dependent. For the base case dose size of 1×10^{14} vg/dose, the required equipment sizes, number of units, and COG/dose (±3%) do not differ significantly when using either material retention method. However, at the lowest dose size evaluated in this study (1×10^{12} vg/

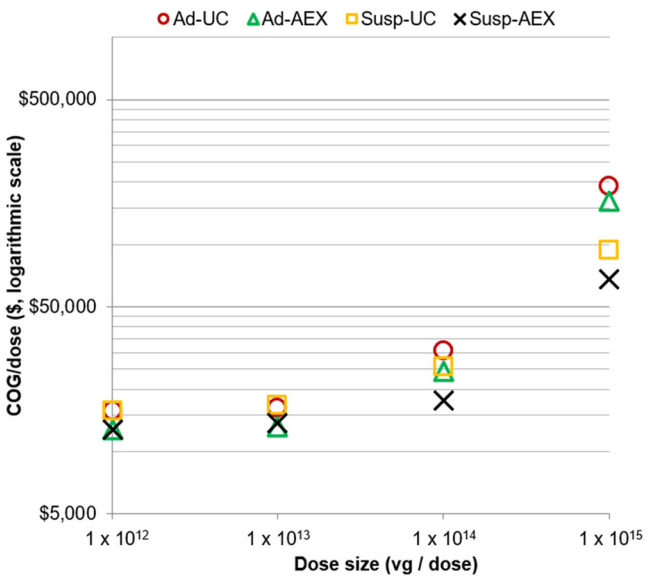

FIGURE 4 Scatter plots displaying the COG/dose change with increasing dose size. The demand was assumed to be 1000 doses/year. The facility was resized for each set of inputs. AEX, anion-exchange chromatography; COG, cost of goods.

10970290, 0, Downloaded from https://onlinelibrary.wiley.com/doi/10.1002/bit.28402 by University College London UCL Library Services, Wiley Online Library on [26/04/2023]. See the Terms and Conditions (https://onlinelibrary.wiley.com/terms-and-conditions) on Wiley Online Library for rules of use; OA articles are governed by the applicable Creative Commons License

dose), the fixed volume method results in more CF10 units or larger bioreactor sizes (e.g., 10 vs. 5 L); however, this does not significantly impact the COG/dose (2%–4% higher).

4.3 | How does uncertainty impact the robustness of the strategies?

The initial deterministic cost comparison highlighted the economic competitiveness offered by Susp-AEX. The study was extended to capture the impact of the perceived greater uncertainties with suspension culture and AEX, reflected in wider distributions for the cell productivities in suspension culture relative to adherent and in the DSP step yields for AEX relative to UC (Table 2). The Monte Carlo simulation technique was used to characterize the impact of these uncertainties on the COG/dose values. The findings from this analysis were assessed in terms of robustness and risk associated with each strategy.

Figure 5a shows the results from the Monte Carlo simulation as COG/dose frequency distributions displayed as violin plots. This illustrates that the uncertainties do not change the ranking found in the deterministic analysis. Overall, the impact of uncertainty was more pronounced in strategies employing less scalable technologies, namely adherent cell culture and UC purification, despite the tighter input distributions upon these variables. Susp-AEX unequivocally achieved the lowest COG/dose and the tightest distribution, as well as the highest probability of meeting any COG/dose target. Furthermore, Ad-UC, Ad-AEX, Susp-UC all resulted in bimodal distributions, whilst Susp-AEX gave a trimodal distribution. Details into the key drivers for the shape of each distribution are outlined below.

In general, for UC-containing strategies, changes in the number of UCs required for purification was the key driving force in defining the shape of the distributions (shown in Supporting Information: Figures S1a and c). The distributions for both Ad-UC and Susp-UC show two distinct peaks, representing the change in the number of

(a)

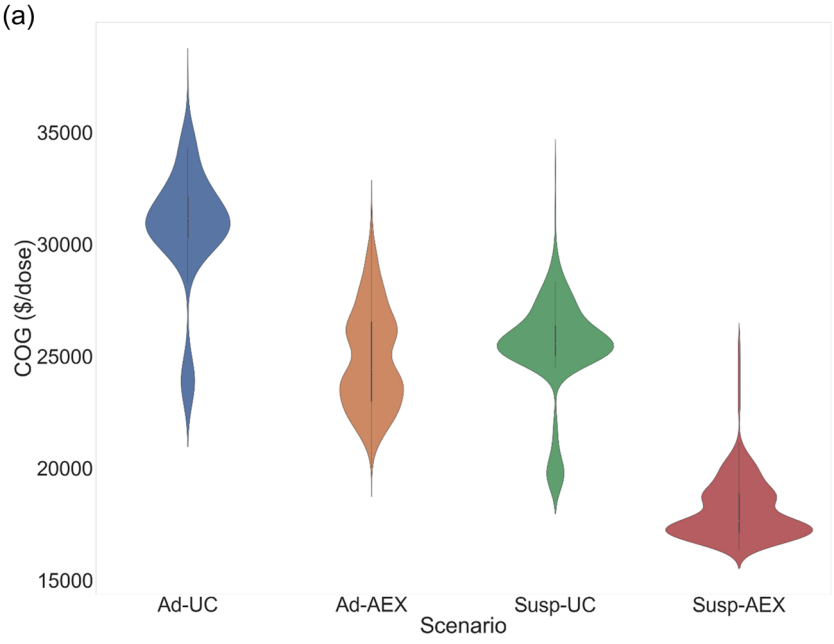

(b)

Scenario	Mean ($/dose)	Standard deviation ($/dose)
Ad-UC	30,017	3,296
Ad-AEX	25,827	2,350
Susp-UC	24,058	2,951
Susp-AEX	18,214	1,537

(c)

Flowsheet	Cell productivity ($x10^5$ vg/cell)	Adherent harvest cell density ($x10^5$ cells/cm^2)	Suspension harvest cell density ($x10^6$ cells/mL)	UC yield (%)	AEX yield (%)
Ad-UC	Tr(1, 1.2, 1.3)	Tr(1.6, 2, 2.4)	N/A	Tr(0.5, 0.7, 0.8)	N/A
Ad-AEX	Tr(1, 1.2, 1.3)	Tr(1.6, 2, 2.4)	N/A	N/A	Tr(0.4, 0.6, 0.8)
Susp-UC	Tr(0.2, 0.6, 1)	N/A	Tr(0.8, 1.0, 1.2)	Tr(0.5, 0.7, 0.8)	N/A
Susp-AEX	Tr(0.2, 0.6, 1)	N/A	Tr(0.8, 1.0, 1.2)	N/A	Tr(0.4, 0.6, 0.8)

FIGURE 5 Uncertainty analysis results from the Monte Carlo simulation showing (a) violin plots of the COG/dose distributions for each scenario aunder uncertainty, (b) key probabilistic output parameters for each scenario, (c) uncertain process input parameters and their distributions evaluated in the Monte Carlo simulations. The demand was assumed to be 1000 doses/year, with a dose size of 1×10^{14} vg/dose. The facility was resized for each set of inputs. AEX, anion-exchange chromatography; COG, cost of goods.

10970290, 0, Downloaded from https://onlinelibrary.wiley.com/doi/10.1002/bit.28402 by University College London UCL Library Services, Wiley Online Library on [26/04/2023]. See the Terms and Conditions (https://onlinelibrary.wiley.com/terms-and-conditions) on Wiley Online Library for rules of use; OA articles are governed by the applicable Creative Commons License

ultracentrifuges required in certain instances. As discussed in the base case analysis and Figure 3, 23 ultracentrifuges were required in parallel, which is represented by the larger peak in Figure 5a for both Ad-UC and Susp-UC. In scenarios where it is possible to achieve higher UC yields or cell culture productivities, the number of UCs needed reduced to 9 (the smaller peak in the UC distributions). This distinct and relatively large drop highlights the sensitivity of UC sizing to changes in key input parameters.

Conversely, for AEX-containing scenarios, changes in USP were shown to be far more significant in driving the shape of the plots (as evidenced by Supporting Information: Figures S1b and d). For Ad-AEX, shown in Supporting Information: Figure S1b, the key factor in determining the distribution shape was found to be the number of incubators required for the many CF10 units used in both seeding and cell culture. Small differences in input parameters such as titers and yield resulted in changes in the number of CF10 units required. As this changes, so does the number of incubators used during USP. In contrast, Susp-AEX COG differences were primarily driven by bioreactor size, giving rise to three peaks as shown in Supporting Information: Figure S1d. At the base case, a 250 L bioreactor was required, however instances where titer and yields fluctuated to lower levels resulted in larger processing volumes, prompting the use of bigger bioreactors, (e.g., 500 and 1000 L). Hence this ultimately gave rise to the trimodal distribution that is displayed.

4.4 | What is the optimal purification strategy in terms of meeting cost and purity targets?

As discussed in Section 1, there are numerous unit operations available for purifying AAV vector products beyond batch UC (batchUC) and AEX; these include other chromatography options. In this study, the pool of purification options was expanded to include multimodal chromatography (MM), cation exchange chromatography (CEX), continuous ultracentrifugation (ContiUC), and a range of affinity chromatography (AFF) resins, with different cost and capacity trade-offs (see Table 3 for full list of options). DBCs reported for affinity resins range from 1×10^{12} to 1×10^{14} vg/mL, however more conservative values were selected to characterize the trade-off between affinity resins, for example, a lower DBC for the lower cost resins and a higher DBC for the higher cost resin. It must be noted that even if the upper end of the reported affinity DBC range was assumed, this would not significantly affect the outcomes, as typically the columns were oversized to reach a GMP size and to avoid longer column loading times.

Due to the breadth of flowsheets that could be constructed from such options, it is desirable to ascertain the most cost-effective of the set evaluated, which can simultaneously satisfy various purity targets. From a purity perspective, there is a lack of well-defined data published on various impurity starting and target removal levels in AAV manufacturing. Subsequently, three heat-maps were generated, one for each impurity investigated (empty capsids, HCPs, and DNA), evaluating a range of potential starting and target levels. Figure 6 displays these heat-maps from assessing the COG/dose and purity of each DSP sequence. Red colored boxes represent more expensive options relative to those that are blue. The gray colored areas represent those options that breach the imposed constraints (see Supporting Information: Figure S2 for the specific constraint labeling on the gray-colored areas). Moreover, solutions that fall within the purple contour represent feasible combinations at the given purity target or starting level.

Figure 6a evaluated three target empty capsid removal levels, with a distinct change in optimal solution shown at each. In scenarios where less than 75% empty capsid removal was achieved, the most economical and hence optimal purification strategy was "AFFH-MM," using an affinity resin with high DBC (AFFH) and a mixed-mode resin. This can be primarily attributed to the high overall yield of the combination relative to other choices. This allowed for a lower overall processing volume at harvest and hence a lower raw materials cost. However, both AFFH and MM do not possess empty capsid removal capabilities since they cannot distinguish between full and empty particles. Thus, this train was not sufficient to meet either the 75% or 90% purity targets. The technologies assumed to be able to make the distinction between full and empty were AEX and UC techniques, thus the higher purity targets were shown to require inclusion of one of these steps. This was first observed for the 75% purity target, where AEX and UC options were sufficient to at least meet this goal. In satisfying both objectives of cost and purity, AEX was shown to be marginally more cost-effective than UC, driven by lower labor costs. Having said this, when moving to the 90% target, AEX became infeasible from a purity perspective and ContiUC was the operation that satisfied both the cost and impurity removal target. ContiUC sizing is based on flowrate, offering a more scalable alternative to the batch counterpart. In general, fully chromatographic platforms or those utilizing ContiUC were shown to be more cost-effective than those using batchUC, reinforcing the importance of scalability. As shown in Figure 6, most purification trains containing batchUC as a capture step were omitted from the optimization due to breaching the equipment constraint. BatchUC was shown to only be feasible as a polishing step coupled with a CEX or AEX capture, due to their high dynamic binding capacities that translate into a lower volume to be processed by UC. Nevertheless, as evidenced by Figure 6, whilst feasible, these options are amongst the least cost-effective of the set, attributable to the requirement for 11 parallel UC units, thereby driving up labor and indirect costs.

When studying HCPs and DNA, the low level (L) for each resulted in AFFH-MM being optimal, (Figure 6b,c). The AFF-MM flowsheet was assumed to be capable of reaching an overall HCP and DNA log reduction value (LRV) of ~7.5 and ~4.5, respectively, which did not meet the target specification. For high starting impurity levels, the optimal strategy that met the purity targets was found to be AFFH-ContiUC for HCPs and AFFH-AEX for DNA. AFFH-ContiUC yielded an HCP LRV of ~8.5, whilst AFFH-AEX was found to have a DNA LRV of ~6.

Also included in the analysis was the option for a three-step purification train, involving the addition of an AEX step after MM, to provide additional purification capabilities. Whilst the three-step using AEX met the higher purity targets (for HCP, DNA, and empty capsids) in contrast to many of the two-step options alone, the three-step

10970290, 0, Downloaded from https://onlinelibrary.wiley.com/doi/10.1002/bit.28402 by University College London UCL Library Services, Wiley Online Library on [26/04/2023]. See the Terms and Conditions (https://onlinelibrary.wiley.com/terms-and-conditions) on Wiley Online Library for rules of use; OA articles are governed by the applicable Creative Commons License

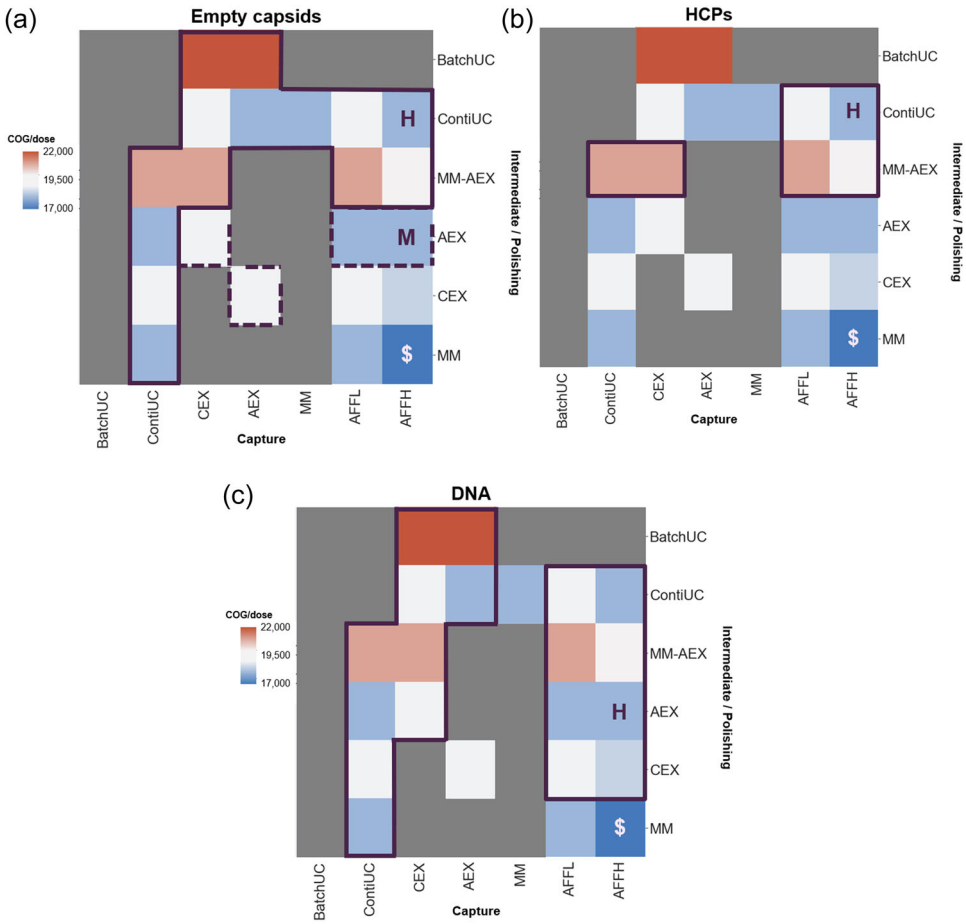

FIGURE 6 Brute-force optimization outputs for AAV capture and polishing scenarios where (a) differing target levels of empty capsid removal are encountered, (b) different starting levels of host cell proteins (HCP), and (c) different starting levels of DNA are defined. The $ symbols represent the most cost-effective option when less than 75% empty capsid removal is achieved or low starting levels of HCP or DNA (2×10^{-7} and 6×10^{-10} ng/vg) are assumed. For (a), M = optimal solution when at least 75% removal of empty capsids is required and H = optimal solution when at least 90% removal of empty capsids are required. For (b) and (c), H = optimal solution when a high impurity load is used (2×10^{-5} and 6×10^{-8} ng/vg). The contours represent the following; (- - -) meet target for a moderate impurity level, (——) meet target for a high impurity level. Gray box = breach constraints (see Supporting Information: Figure S2 for details on constraints). The demand was assumed to be 1000 doses/year, with a dose size of 1×10^{14} vg/dose. The facility was resized for each set of inputs.

purification trains were found to be less cost-effective than AFFH-ContiUC. This observation highlights that three-step trains are only necessary if employing AFFH-ContiUC is not an available option, reinforcing its cost effectiveness and impurity removal capabilities.

Although, ContiUC was shown to be the optimal polishing choice when simultaneously considering cost and purity, it must be noted that there are still challenges surrounding its implementation and use in commercial AAV manufacturing. Despite its scalability, ContiUC is relatively less well-understood than its non-scalable counterpart, batch UC. Additionally, unlike chromatography, ContiUC is not industrially established as a purification option for AAV and as a result, may require a larger process development effort initially when integrating into a manufacturing process. Furthermore, ContiUC generally requires establishment and maintenance of a stable density gradient at the large-scale to recreate the environment encountered in the batch ultracentrifuge, thus requiring additional process optimization and characterization studies. Finally, the reliance on niche chemicals such as iodixanol may prove limiting in terms of throughput due to ongoing supply chain issues. As a result, further work is likely required to identify suitable materials and consistent supply for large-scale application and sourcing.

The potential of the technology is significant however, as it enables scale-up based on a similar separation principle when moving from the relatively well-characterized batch UC. Furthermore, the ability for ContiUC to evade the scalability limitations of batch is advantageous for future commercial implementation, particularly as the product loading potential is up to 40 times the actual rotor volume.

4.5 | How does the optimal polishing strategy change with AEX yield and empty capsid removal?

As alluded to in the uncertainty analysis section of the case study, there are several uncertain process parameters or targets

10970290, 0, Downloaded from https://onlinelibrary.wiley.com/doi/10.1002/bit.28402 by University College London UCL Library Services, Wiley Online Library on [26/04/2023]. See the Terms and Conditions (https://onlinelibrary.wiley.com/terms-and-conditions) on Wiley Online Library for rules of use; OA articles are governed by the applicable Creative Commons License

(a)

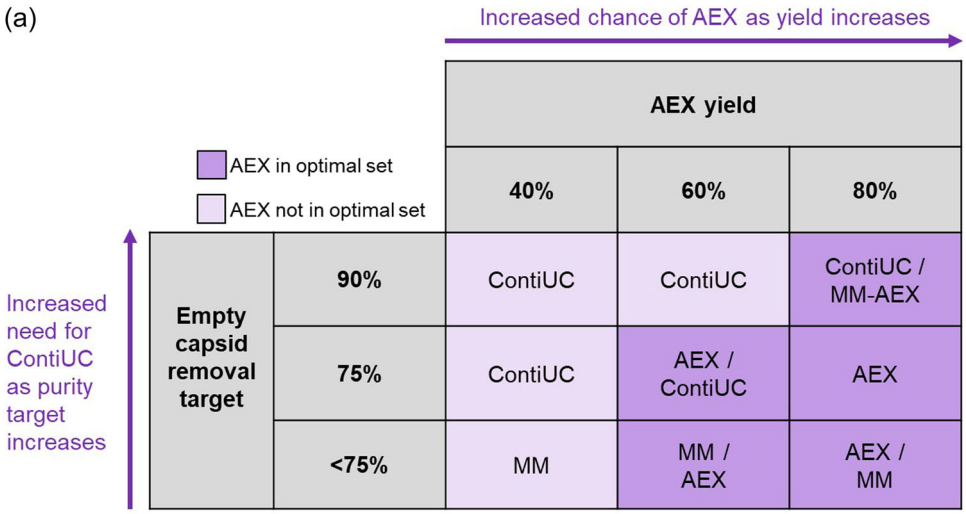

(b)

Empty capsid removal target	Feasible polishing options					
	MM	CEX	AEX	ContiUC	BatchUC	MM-AEX
90%	Y	Y	Y	Y	Y	Y
75%	N	N	Y	Y	Y	Y
<75%	N	N	N	Y	Y	Y

FIGURE 7 (a) Optimal polishing purification choice in terms of COG/g across a matrix of scenarios with different combinations AEX yields and purity targets. An "/" sign in each box is used to represent solutions that fall within a 5% COG/dose difference from the optimal solution. Lighter shading represents solutions that do not contain AEX in the winning solution. Darker shading represents solutions that do contain AEX in the winning solution. (b) Feasible solutions remaining in brute-force optimization choices at each purity target. The demand was assumed to be 1000 doses/year, with a dose size of 1×10^{14} vg/dose. The facility was resized for each set of inputs. AEX, anion-exchange chromatography; COG, cost of goods.

associated with AAV processing. To capture this variability encountered in AAV manufacturing, the AEX yield was varied for different empty capsid removal targets. Figure 7a shows the resulting matrix of optimal solutions for different combinations. Figure 7a highlights that AEX yield has a significant impact on the choice of optimal solution. At AEX yields of 60% (base case) and 80%, AEX was preferred at the low and medium purity targets but was unable to compete at the high purity target with ContiUC. Nevertheless, at the 80% yield, a three-step chromatography-based alternative to ContiUC, featuring AEX, was shown to be competitive with ContiUC. Equivalence in this case was defined as two options having a COG/dose with less than 5% difference between them. However, if the AEX yield were to drop to 40% as some have reported (see Supporting Information: Table S1), this would result in AEX being unable to compete at all, with it failing to feature across any of the purity targets. Such a drop pushes up the resin volume required and hence leads to a higher materials cost. As a result, the optimal solution shifts to either MM or ContiUC depending on the purity target required.

Furthermore, as the purity target increases, the remaining feasible solution set reduces, as many platforms cannot meet the empty capsid removal requirement (Figure 7b). The effect of this can be observed when moving to the 75% target, where the key competitor to AEX, which was MM polishing, was removed as a feasible option. As outlined in Figure 6, AEX polishing (two-step) was not sufficient to meet the 90% removal target. As such, UC or three-step AEX was necessary to be included in the purification train due to their propensity for removing empty capsids. In this instance, as evidenced by Figure 7b, the feasible polishing steps remaining at this purity target were batch or ContiUC or three-step AEX. ContiUC was shown to be the most cost-effective across all AEX yields and additionally MM-AEX became more competitive at the higher AEX yield.

In summary, it was shown that where higher AEX yields were achievable, the optimal polishing solution shifted toward the inclusion of AEX, making it more attractive and competitive with other possible options. Nevertheless, the trade-off still exists between reaching higher purities with scalable technologies, whilst implementing robust unit operations that exhibit minimal yield variations between serotypes. Therefore, whilst AEX is known to be a scalable option, the wide range of yields that can be encountered may lead to reductions in cost-effectiveness relative to competing technologies and preference for more yield-stable polishing stages such as ContiUC in some instances.

10970290, 0, Downloaded from https://onlinelibrary.wiley.com/doi/10.1002/bit.28402 by University College London UCL Library Services, Wiley Online Library on [26/04/2023]. See the Terms and Conditions (https://onlinelibrary.wiley.com/terms-and-conditions) on Wiley Online Library for rules of use; OA articles are governed by the applicable Creative Commons License

5 | CONCLUSION

This paper presented the use of a decisional tool for the evaluation of AAV manufacturing processes, first evaluating a small decision space, before use of an optimization algorithm to expand the solution set and find the optimal in terms of cost-effectiveness and meeting purity targets. The deterministic analysis focused upon comparison at key points in the process, namely addressing issues of scalability at USP and during purification. This analysis highlighted the economic superiority of a suspension cell culture strategy over an adherent one, as well as of AEX chromatography over iodixanol gradient ultracentrifugation, with the flowsheet combining suspension culture and AEX chromatography attaining a COG/dose below $20,000 at 1000 doses per year. The impact of AAV dose (and hence chosen disease area) upon process economics illustrated that adherent and suspension culture can offer similar costs at lower doses but, at higher doses, strategies utilising suspension culture are clearly cheaper.

The case study also incorporated an uncertainty analysis using Monte Carlo simulation to identify key risks associated with undertaking the various strategies. It was found that the strategy using adherent culture with AEX chromatography produced the widest distribution, and, hence had the most risk associated with it. This was attributable to the wider input yield distribution associated with AEX and the impact this has on adherent culture sizing. The risk associated with AEX suggested that for manufacturers utilizing the traditional AAV platform (adherent culture with ultracentrifugation), if a minimal process switch is initially desired, then efforts should be focussed upon a USP switch first over DSP, for a more cost-effective and robust initial outcome.

The optimization case study reinforced the cost-effectiveness of scalable purification platforms, however also revealed the distinct sensitivity that purification performance had on the optimal choice. The purification sequence of affinity followed by multimodal chromatography was deemed the optimal solution at the low starting or target impurities levels, whereas affinity chromatography with continuous ultracentrifugation was found to be the best combination at high levels. This was similarly seen when varying AEX yield. The decisional tool therefore served as a strategy to rapidly assess a myriad of AAV manufacturing options, accounting for both economics and purity to derive optimal solutions.

AUTHOR CONTRIBUTIONS

Annabel Lyle: Conceptualization, data curation, formal analysis, investigation, visualization, modeling, methodology, paper writing (original draft and review and editing). **Suzanne Farid:** Conceptualization, funding acquisition, resources, supervision, visualization, validation, writing (review and editing). **Christos Stamatis:** Resources, supervision, modeling, visualization, writing (review and editing). **Martyn Hulley:** Resources, supervision, and validation. **Thomas Linke:** Resources, supervision, and validation. **Albert Schmelzer:** Resources, supervision, and validation. **Richard Turner:** Conceptualization, resources, supervision, and validation.

ACKNOWLEDGMENTS

The author would like to thank the following industrialists for sharing their experience on AAV manufacturing: Lekan Daramola, Clive Glover, and Jim Mills. Financial support from AstraZeneca and the UK Engineering and Physical Sciences Research Council (EPSRC) is gratefully acknowledged (EngD Grant Code: EP/S021868/1). UCL Biochemical Engineering hosts the Future Targeted Healthcare Manufacturing Hub in collaboration with UK universities and with funding from the EPSRC and a consortium of industrial users and sector organizations.

DATA AVAILABILITY STATEMENT

The data that support the findings of this study are available from the corresponding author upon reasonable request.

ORCID

Annabel Lyle http://orcid.org/0000-0002-6629-9522
Christos Stamatis http://orcid.org/0000-0003-1761-567X
Suzanne S. Farid http://orcid.org/0000-0001-8155-0538

REFERENCES

Bracewell, D. G., Francis, R., & Smales, C. M. (2015). The future of host cell protein (HCP) identification during process development and manufacturing linked to a risk-based management for their control. *Biotechnology and Bioengineering*, *112*(9), 1727–1737. https://doi.org/10.1002/BIT.25628

Bulcha, J. T., Wang, Y., Ma, H., Tai, P., & Gao, G. (2021). Viral vector platforms within the gene therapy landscape. *Signal Transduction and Targeted Therapy*, *6*(1), 53. https://doi.org/10.1038/s41392-021-00487-6

Cameau, E., Pedregal, A., & Glover, C. (2020). Vector channel: Adherent cost modelling comparison of adherent multi-trays with suspension and fixed-bed bioreactors for the manufacturing of gene therapy products. *Cell & Gene Therapy Insights*, *5*(11), 1663–1675. https://doi.org/10.18609/cgti.2019.175

Chen, H., Marino, S., & Ho, C. Y. (2016). 97. Large scale purification of AAV with continuous flow ultracentrifugation. *Molecular Therapy*, *24*, S42. https://doi.org/10.1016/s1525-0016(16)32906-9

Comisel, R. M., Kara, B., Fiesser, F. H., & Farid, S. S. (2021a). Gene therapy process change evaluation framework: Transient transfection and stable producer cell line comparison. *Biochemical Engineering Journal*, *176*(May), 108202. https://doi.org/10.1016/j.bej.2021.108202

Comisel, R. M., Kara, B., Fiesser, F. H., & Farid, S. S. (2021b). Lentiviral vector bioprocess economics for cell and gene therapy commercialization. *Biochemical Engineering Journal*, *167*, 107868. https://doi.org/10.1016/j.bej.2020.107868

Crosson, S. M., Dib, P., Smith, J. K., & Zolotukhin, S. (2018). Helper-free production of laboratory grade AAV and purification by iodixanol density gradient centrifugation. *Molecular Therapy. Methods & Clinical Development*, *10*, 1–7. https://doi.org/10.1016/j.omtm.2018.05.001

Dobrowsky, T., Gianni, D., Pieracci, J., & Suh, J. (2021). AAV manufacturing for clinical use: Insights on current challenges from the upstream process perspective. *Current Opinion in Biomedical Engineering*, *20*, 100353. https://doi.org/10.1016/j.cobme.2021.100353

Glover, C., Smith, D., & Marshall, D. (2019). Room for improvement: Tackling suboptimal downstream process unit operations for viral vectors. *Cell and Gene Therapy Insights*, *5*(S2), 165–176. https://doi.org/10.18609/cgti.2019.024

10970290, 0, Downloaded from https://onlinelibrary.wiley.com/doi/10.1002/bit.28402 by University College London UCL Library Services, Wiley Online Library on [26/04/2023]. See the Terms and Conditions (https://onlinelibrary.wiley.com/terms-and-conditions) on Wiley Online Library for rules of use; OA articles are governed by the applicable Creative Commons License

Hebben, M. (2018). Downstream bioprocessing of AAV vectors: Industrial challenges & regulatory requirements. *Cell and Gene Therapy Insights*, *4*(2), 131–146. https://doi.org/10.18609/cgti.2018.016

van der Loo, J. C. M., & Wright, J. F. (2016). Progress and challenges in viral vector manufacturing. *Human Molecular Genetics*, *25*(R1), R42–R52. https://doi.org/10.1093/hmg/ddv451

Masri, F., Cheeseman, E., & Ansorge, S. (2019). Viral vector manufacturing: How to address current and future demands? *Cell and Gene Therapy Insights*, *5*(S5), 949–970. https://doi.org/10.18609/cgti.2019.104

Nass, S. A., Mattingly, M. A., Woodcock, D. A., Burnham, B. L., Ardinger, J. A., Osmond, S. E., Frederick, A. M., Scaria, A., Cheng, S. H., & O'Riordan, C. R. (2018). Universal method for the purification of recombinant AAV vectors of differing serotypes. *Molecular Therapy. Methods & Clinical Development*, *9*, 33–46. https://doi.org/10.1016/j.omtm.2017.12.004

Pereira Chilima, T. D., Moncaubeig, F., & Farid, S. S. (2020). Estimating capital investment and facility footprint in cell therapy facilities. *Biochemical Engineering Journal*, *155*, 107439. https://doi.org/10.1016/j.bej.2019.107439

Qu, W., Wang, M., Wu, Y., & Xu, R. (2015). Scalable downstream strategies for purification of recombinant adeno-associated virus vectors in light of the properties. *Current Pharmaceutical Biotechnology*, *16*(8), 684–695. https://doi.org/10.2174/1389201016666150505122228

Simaria, A. S., Turner, R., & Farid, S. S. (2012). A multi-level meta-heuristic algorithm for the optimisation of antibody purification processes. *Biochemical Engineering Journal*, *69*, 144–154. https://doi.org/10.1016/J.BEJ.2012.08.013

Stamatis, C., & Farid, S. S. (2021). Process economics evaluation of cell-free synthesis for the commercial manufacture of antibody drug conjugates. *Biotechnology Journal*, *16*(4), 2000238. https://doi.org/10.1002/biot.202000238

Wang, C., Mulagapati, S. H. R., Chen, Z., Du, J., Zhao, X., Xi, G., Chen, L., Linke, T., Gao, C., Schmelzer, A. E., & Liu, D. (2019). Developing an anion exchange chromatography assay for determining empty and full capsid contents in AAV6.2. *Molecular Therapy. Methods & Clinical Developmen.t*, *15*(December), 257–263. https://doi.org/10.1016/j.omtm.2019.09.006

Wright, J. F. (2008). Manufacturing and characterizing AAV-based vectors for use in clinical studies. *Gene Therapy*, *15*(11), 840–848. https://doi.org/10.1038/gt.2008.65

Wright, J. F (2020). Quality control testing, characterization and critical quality attributes of adeno-associated virus vectors used for human gene therapy. https://doi.org/10.1002/biot.202000022

Wright, J. F. (2014a). AAV empty capsids: For better or for worse? *Molecular Therapy*, *22*(1), 1–2. https://doi.org/10.1038/mt.2013.268

Wright, J. F. (2014b). Product-related impurities in clinical-grade recombinant AAV vectors: Characterization and risk assessment. *Biomedicines*, *2*, 80–97. https://doi.org/10.3390/biomedicines2010080

Xiao, X., Li, J., & Samulski, R. J. (1998). Production of high-titer recombinant adeno-associated virus vectors in the absence of helper adenovirus. *Journal of Virology*, *72*(3), 2224–2232. http://www.ncbi.nlm.nih.gov/pubmed/9499080

SUPPORTING INFORMATION

Additional supporting information can be found online in the Supporting Information section at the end of this article.

How to cite this article: Lyle, A., Stamatis, C., Linke, T., Hulley, M., Schmelzer, A., Turner, R., & Farid, S. S. (2023). Process economics evaluation and optimization of adeno-associated virus downstream processing. *Biotechnology and Bioengineering*, 1–14. https://doi.org/10.1002/bit.28402

10970290, 0, Downloaded from https://onlinelibrary.wiley.com/doi/10.1002/bit.28402 by University College London UCL Library Services, Wiley Online Library on [26/04/2023]. See the Terms and Conditions (https://onlinelibrary.wiley.com/terms-and-conditions) on Wiley Online Library for rules of use; OA articles are governed by the applicable Creative Commons License